Biological and Biomedical Journal

Journal homepage: https://bbj.journals.ekb.eg

Ameliorative efficacy of the sea cucumber *Holothuria polii* extract against the hepato-renal and lung toxicity induced by cyclophosphamide in adult male albino rat

Noha M. Samak*, Salwa A. El-Saidy, Gihan M. Elkhodary, Hadeer M. El-Sayed

Zoology Department, Faculty of Science, Damanhur University, Egypt

ARTICLE INFO

Received: 30/1/2025
Revised: 17/4/2025
Accepted: 1/5/2025

Corresponding author:
Noha M. Samak, Ph. D
E-mail: noha.samak@sci.dmu.edu.eg
Mobile: 01005301157

P-ISSN: 2974-4334
E-ISSN: 2974-4324
DOI: 10.21608/BBJ.2025.382456.1102

ABSTRACT

Cyclophosphamide (CTX) treatment for cancer has serious adverse effects on the liver, kidney, lungs, and other organs. This study evaluated the efficacy of *Holothuria polii* extract (HPE) in ameliorating liver, kidney, and lung tissues recovery from CTX-induced toxicity in rats' model. The experimental rats were randomly divided into four groups (10 rats for each) as follows: Group 1 (Gp1) was served as a control group. In Gp2, rats were administered HPE (3.8 mg/kg b.wt) orally/day for eight consecutive days. Gp3, rats were received a single dose of CTX (200 mg/kg b.wt.) intraperitoneally (i.p.) injected. Gp4 rats were injected with CTX as in Gp3 and administered orally with HPE as in Gp2. Aspartate and alanine aminotransferases, albumin, total bilirubin, uric acid, creatinine, superoxide dismutase, catalase, glutathione reduced, malondialdehyde, angiotensinogen, angiotensin II, renin, aldosterone, tumor necrotic factor-α, interleukin-1 beta, caspase 3 and minerals were measured. Investigations were conducted on histological changes in the liver, kidney, and lung tissues. According to the findings, rats' liver, kidney, and lung histological structures and normal functioning were all changed by CTX injections. HPE treatment post CTX injection improves histological structure and physiological functions.

Keywords: Antioxidant, Anti-inflammation, Cyclophosphamide Hepato-renal toxicity, *Holothuria polii extract*, Lung toxicity

1. Introduction

One common alkylating chemotherapeutic drug is cyclophosphamide (CTX), which is used to treat autoimmune disorders and a variety of malignancy (Mills et al., 2019). CTX is a member of the nitrogen mustard class of alkylating compounds. A phosphoramide group in its chemical structure is essential to its bioactivation (Teng and Wang, 2025). It is widely used to treat a variety of cancers, especially solid tumors and hematologic cancers. Leukemias, breast, small cell lung, ovarian, multiple myeloma cancer, Hodgkin and non-Hodgkin lymphoma are all treated with CTX (Huang et al., 2020). CTX is used in conjunction with immunotherapies like checkpoint inhibitors, at low dosages, it decreases regulatory T cells, which improves the immune response to malignancies (Mamede et al., 2024). In addition to these positive outcomes, CTX has been linked to a number of negative side effects, including genotoxicity and lung fibrosis (Boopathi and Thangavel, 2021). A crucial component of preconditioning protocols for bone marrow and hematopoietic stem cell transplantation, CTX functions as an immunosuppressive agent to treat severe autoimmune diseases (Gao et al., 2024). This suppression makes people more vulnerable to infections, anemia, and bleeding (Nian et al., 2024). The P450 enzyme system in the liver transforms the prodrug CTX into active metabolites. Furthermore, it may act as an autoinducer of the enzymatic system. Acrolein and mustard phosphoramide are the two active metabolites of CTX. The antineoplastic and cytotoxic actions of CTX are produced by phosphorylamide mustard, while acrolein

produces additional toxic effects. Acrolein promotes the production of free radicals and triggers the harmful effects, whereas phosphorylamide mustard works by binding to DNA and stopping cell division (Gungor et al., 2023). There have been reports of interstitial pneumonitis and pulmonary fibrosis in patients receiving CTX. Despite being very uncommon, the occurrence has the potential to cause long-term respiratory damage (Li et al., 2025). Interstitial pneumonitis, which is characterized by inflammation of the lung's interstitial tissue, can be brought on by CTX. The activation of inflammatory cytokines, like tumor necrosis factor (TNF) -α and interleukin (IL) -6, by this oxidative stress leads to lung cell death and tissue damage (Rivera-Lazarín et al., 2024). Immunosuppression brought on by CTX weakens the lung's defenses, making patients more vulnerable to infections such as bacterial pneumonia and *Pneumocystis jirovecii* pneumonia. In addition to causing inflammation, these infections can exacerbate lung damage (Brandi and Frega, 2019). Alveolar wall thickening, inflammatory cell infiltration, and fibrosis are examples of histological alterations.

CTX can cause hepatotoxicity, which includes increased liver enzymes and liver damage. The therapeutic dosage of CTX may cause hepatic toxicity (El-Naggar et al., 2016). Treatment with CTX can affect the liver's ability to detoxify and produce bile, which can lead to cholestasis. After receiving CTX, hepatic enzyme abnormalities were detected, indicating potential liver injury. These enzymes include serum alanine and aspartate aminotransferases (ALT and AST), and alkaline phosphatase (Polak et al., 2024). CTX is known as nephrotoxic agent, as is its metabolite acrolein. They cause glomerular damage, interstitial inflammation, and acute tubular necrosis. Following CTX treatment, there were reports of decreased glomerular filtration rate, poor waste elimination that resulted in urea buildup, creatinine, electrolyte imbalances, and an elevated risk of acute kidney injury (Liang et al., 2023). Natural products, especially marine products, have gained attention for their therapeutic and preventive potential because of their bioactive components that have immunomodulatory, anti-inflammatory, and antioxidant qualities (Elbandy, 2022). These substances have shown protective benefits against CTX-induced oxidative stress (Rajauria et al., 2016). Sea cucumbers are marine invertebrates that are found to be well distributed worldwide and have high economic and food value (Hossain et al., 2020). The therapeutic capabilities and medicinal advantages of sea cucumbers are attributable to a diverse range of secondary metabolites, which not only protect them from predators but also offer significant therapeutic and medicinal benefits (Kamyab et al., 2020; Omran et al., 2020).

Holothuria polii (Delle Chiaje, 1823) (Order: Aspidochirotida, and Family: Holothuriidae) is one of the most abundant sea cucumber species in the Mediterranean Seashore (Moussa and Wirawati, 2018). It has a brown-colored cylindrical body spotted with dark brown spots. Its therapeutic importance has been investigated in many previous studies that have shown that extracts of *H. polii* sea cucumber have important bioactive components, exhibiting pharmacological activities like antifouling, antimicrobial, antiparasitic, anticoccidial, anti-inflammatory, anti-proliferative, and antitumor properties (Omran and Khedr, 2015; Ozupek and Cavas, 2017; Kareh et al., 2018; El-Saidy et al., 2024; El-Sayed et al., 2024; Mohamed et al., 2024; Wingfield et al., 2024). Reducing inflammation and oxidative stress by natural products, led to shield the liver and kidney against CTX-induced damage (Cao et al., 2022). Although several studies have been published on *H. polii* extract (HPE) bioactivities, limited information exists on the protective efficacy of HPE against chemotherapy-induced toxicity. For this reason, the present study was conducted to evaluate the protective effect of HPE treatment against CTX-induced injury in liver, kidney, and lung tissues in experimental male rats.

2. Materials and methods

Chemicals

Sigma-Aldrich Chemicals Co., located in St. Louis, MO, USA, was the supplier of CTX. The experimental rats received intraperitoneal (i.p.) injections of CTX that had been dissolved in standard saline solutions.

Sampling and characterization of the sea cucumber *H. polii*

Twenty specimens of sea cucumber *H. polii* were collected by self-contained underwater breathing apparatus diving from the intertidal region at Abu-Qir, along the Alexandria coast, Egypt. The taxonomic identification of the samples was based on their morphometric and morphological characteristics and the shape of the ossicles according to studies of El-Saidy *et al.* (2024). Specimens were transported in plastic containers to the laboratory within 2 h. The samples were cleaned with distilled water and dissected to remove all internal viscera. Then, the body wall was cut into small pieces (< 1 cm^2) and freeze-dried at –20°C until used in extraction.

Holothuria polii crude extract preparation

The ethanolic extract was conducted from the body wall of *H. polii*. The extract was prepared according to Mona et al. (2012) and El-Saidy et al. (2024). In brief, the freeze-dried body wall of the sea cucumber was homogenized using a blender with 95% ethanol (1:4, *w/v*). The extraction was done at room temperature (25°C) for 72 h in the dark with constant shaking. The extract was filtered using a Buchner funnel, concentrated using a vacuum rotary evaporator at 40°C, and then lyophilized. The residual dried extract was kept at –80°C until later usage.

Gas chromatography-mass spectrometry investigation of crude extract from *H. polii*

According to a method described by Ismail et al. (2019) with some modifications, GC-MS analysis of *H. polii* crude extract was conducted utilizing a GC-MS spectrometer (Perkin Elmer model: Clarus 580/560S) fitted with an Elite-5MS column (30 m length, 0.25 mm internal diameter, and 0.25 µm film thickness). The oven temperature was initially held at 80°C for 8 min, 10°C /min to 200°C, held 0 min, and then increased by 5°C /min to 260°C, held 3 min. The injector temperature was kept at 280°C, and the GC-MS analysis was conducted by injecting 1.0 µL of the sample. The mass spectrometer was configured to function in electron impact mode at 70 eV, scanning a range from 40 to 550 Da. Helium served as the carrier gas, compressed to 2223 psi, with a flow rate of 122 mL/min. The identification of components relied on comparing the resultant mass spectra with entries in a mass spectral database library utilized by the GC-MS instrument.

Experimental animals

The study was performed on 40 healthy Wister adult male albino rats (weighted from 160 to 165 g, 11-12 weeks of age). Rats were purchased from the National Research Centre (NRC) in Giza, Egypt, and housed in well-ventilated cages, at room temperature 26 ± 2°C and humidity of 58 ± 5% under 12 hr dark-light cycle for 10 days before the experiment. The experimental protocols follow the Guidelines used for Animal Experimentation and approved by the ethical committee of the Faculty of Science at Damanhur University, Egypt (DMU-SCI-CSRE-24-11-07). Animals were fed standard diet with free access to water *ad libitum*. Animals were carefully observed every day and their body weights, while food consumption and water intakes were measured precisely every day to evaluate any signs of toxicity or abnormality during the experiment.

Experimental design

Ten rats were randomly assigned to each of the four groups of experimental rats. Group 1 (Gp1), the control group, rats were not given any medication. Gp2: Rats administered an oral dose of HPE of dose 3.8 mg/kg/day. This dose is 1/10 of the median lethal dose (LD_{50}) after the conversion of the LD_{50} value of acute oral toxicity in mice reported in Mona et al. (2012) to LD_{50} in rats based on the table of surface-area ratios of some common laboratory species and man (Paget, 1964). The dry extract was suspended in distilled water and administered orally for 7 days. Gp3: Rats received a single i.p. injection of CTX (200 mg/kg b.wt) (Alsemeh and Abdullah, 2022). Gp4: Rats were given an injection of CTX, as the recommended dose of Gp3, and HPE orally as the recommended dose of Gp2. The experimental protocol concluded with all rats being euthanized after 24 hours of fasting, i.p. injection with sodium pentobarbital, and exposed to complete necropsy. Blood samples from rats were collected in two test tubes; the first tube was non-herpanized and second tube herpanized. The sera and plasma were separated, collected and stored at -80°C.

Biochemical analysis, pro-inflammatory cytokines, apoptotic marker, angiotensinogen, renin, angiotensin-II and aldosterone were determined in sera, while antioxidant biomarkers and oxidative biomarkers were measured in plasma. For histopathological examination, liver, kidney and lung tissues were collected and sectioned in 10 % buffered formalin.

Biochemical analysis

Determination of liver and kidney function

All liver function tests were determined in the serum. The activity of ALT (EC 2.6.1.2.) and AST (EC 2.6.1.1.) were colorimetricaly estimated by the recommended procedures of the commercial kits of Biodiagnostic Company, Egypt (CAT. No. AL 10 31 and AS 10 61, respectively). Albumin and total bilirubin were colorimetricaly determined by using the Kits of Biodiagnostic Company (CAT. No. AB 10 10 and BR 11 11, respectively). Creatinine and Uric acid levels were estimated by using the kits of Biodiagnostic Company (CAT. No. CR 12 51 and UA 21 20, respectively).

Determination of electrolytes levels

Sodium (Na), potassium (K), calcium (Ca), chloride (Cl), and magnesium (Mg) levels were measured at wavelengths 545 nm, 420 nm, 585 nm, 456 nm, and 520 nm, respectively, by using colorimetric method by the kits of Biodiagnostic kit (CAT. No. SO 19 10, PT 18 20, CA 12 10, CL 12 11 and MG 16 10, respectively).

Determination of antioxidant markers

The levels activities of superoxide dismutase (SOD, EC 1.15.1.1) and catalase (CAT, E.C. 1.11.1.1.6) enzymes were estimated by using Biodiagnostic kit (CAT. No. SD 25 21 and CAT. No. SD 25 17, respectively). Reduced glutathione (GSH) level was measured by using Biodiagnostic kit (CAT. No. GR 25 11). Malondialdehyde (MDA) level was determined by using Biodiagnostic kit (CAT. No. MD-2529).

Determination of pro-inflammatory cytokines and apoptotic markers

TNF-α was assessed by ELISA method, using appropriate commercial kits from CUSABIO (Houston, TX 77054, USA) with CAT. No. CSB-E11987r. IL-1β was measured by ELISA method, using appropriate commercial kits from BT LAP Company (Jiaxing, Zhejiang Province, China) with CAT. No. E0119Ra. The apoptotic marker caspase-3 was determined by using ELISA Kit from CUSABIO with CAT. No. CSB-E08857r.

Determination of angiotensinogen, renin, angiotensin-II, and aldosterone

By using ELISA method angiotensinogen was determined by using IBL Company (Gunma, Japan) with CAT. No.27414. The aldosterone was determined by using ELISA method according to MyBioSource Company (San Diego, CA, USA) with CAT. No. MBS731388. Angiotensin-II and renin were estimated by using ELISA method according to Kamiya Biomedical Company, Seattle, WA, USA (CAT. No. KT-6638 and CAT. No. KT-60668, respectively)

Histological investigations

The tiny fragments of liver (Drury and Wallington 1980), kidney and lung tissues that had been obtained were immediately preserved for 24 hours in 10% neutral buffered formalin. The tissue samples were dehydrated in increasing grades of ethyl alcohol, clarified by xylene, and embedded in paraffin wax after being cleaned to get rid of any excess fixative. For histological analysis, 5 um thick sections were mounted and stained using the hematoxylin and eosin technique (Tawfiek, 2016).

Statistical analysis

All Data presented as mean ± SD, one–way analysis of variance (ANOVA) was applied to determine the significant differences among different treatments. If there is a significant difference between means, Tukey's *post - hoc* comparisons among different groups were performed. Means that do not share a letter are significantly different (Tukey's test, $p< 0.05$). For all statistical tests p value > 0.05 was considered not statistically significant. p value< 0.05 was considered statistically significant. P value < 0.001 was considered statistically highly significant. GraphPad Prism V. 8.3, IBM SPSS Statistics for Windows, Version 27, and Microsoft Excel 365 (Microsoft Corporation, USA) were used to analyze all of the data.

3. Results

Bioactive compounds in *H. polii* extract

As shown in Fig.1 HPE presented different chemical constituents at different retention times. Palmitic acid is the most abundant compound in HPE followed by octadecanoic acid, 2-bromo dodecane, and hexadecane with peak areas of 4.793, 2.569, 1.869, and 1.089%, respectively.

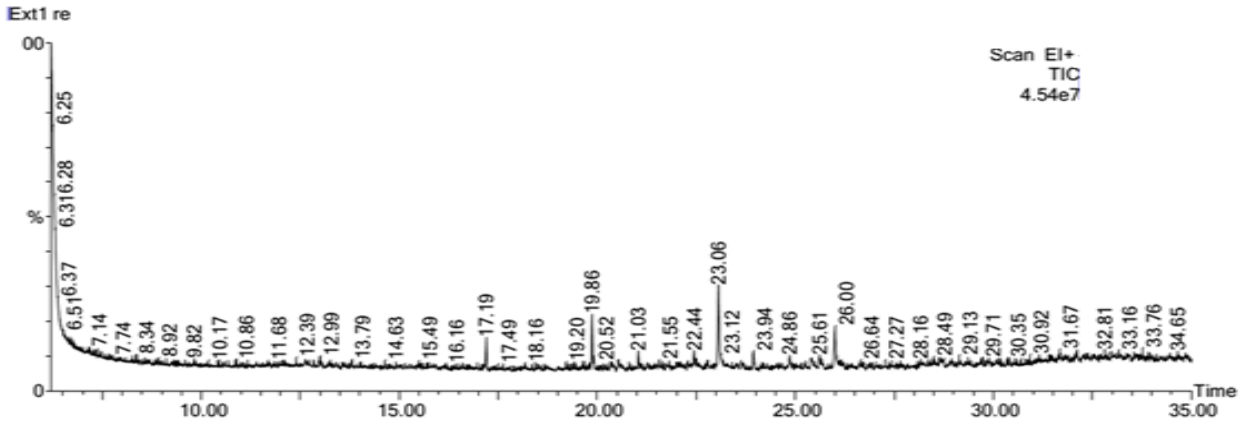

Fig. 1. GC-MS chromatogram of HPE showing the retention times of the identified compounds.

Table.1. Chemical constituents detected in HPE using gas chromatography-mass spectrometry (GC-MS)

Compound name	Compound	Molecular formula	MW (g/mol)	RT (min)	Height	Area (IU)	Area %
Ethyne, fluoro-	Alkyne	C_2HF	44.03	12.001	889635	35215.9	0.31
N,N-Dimethylaniline	Tertiary amine and a dimethylaniline	$C_8H_{11}N$	121.18	12.626	986448	42569	0.37
5-Cyclopropylcarbonyloxypentadecane	Fatty acid ester	$C_{19}H_{36}O_2$	296.5	13.006	1489820	46406.1	0.41
N-Methyltaurine	Aminosulfonic acid	$C_3H_9NO_3S$	139.18	13.406	915801	36364.2	0.32
Trifluoroacetic acid, 2-tetrahydrofurylmethyl ester	Fluoroalkyl ester of a tetrahydrofuran carboxylic acid	$C_7H_9F_3O_3$	198.14	13.811	1098748	34603.8	0.30
Phosphine, ethyl-	Primary phosphine	C_2H_7P	62.05	14.632	1145402	30604.9	0.27
7-Aminoflunitrazepam	Benzodiazepine	$C_{16}H_{14}FN_3O$	283.30	15.907	756358	30855.2	0.27
Dodecane, 5,8-diethyl-	Alkane	$C_{16}H_{34}$	226.44	17.138	888478	28215.3	0.24
Hexadecane	Alkane hydrocarbon	$C_{16}H_{34}$	226.44	17.193	4471546	123213.7	1.09
Sulfurous acid, 2-ethylhexyl hexyl ester	Ester	$C_{14}H_{30}O_3S$	278.45	18.658	920293	28181.2	0.24
2-Bromo dodecane	Bromoalkane	$C_{12}H_{25}Br$	249.23	19.864	7327907	211517.5	1.89
Sulfurous acid, hexyl undecyl ester	Ester	$C_{17}H_{36}O_3S$	320.5	19.909	1926030	43843.2	0.38
Di-n-decylsulfone	Sulfone	$C_{20}H_{42}O_2S$	346.6	20.369	1291334	55686.5	0.49
Chlorozotocin	Nitrosourea	$C_9H_{16}ClN_3O_7$	313.69	20.419	962511	32572.6	0.28
Myristic acid (Tetradecanoic acid)	Saturated fatty acid	$C_{14}H_{28}O_2$	228.37	20.539	1452323	53424	0.47
Sulfurous acid, pentyl undecyl ester	Ester	$C_{16}H_{34}O_3S$	306.5	20.594	936183	33653	0.29
Heptadecane, 2,6-dimethyl-	Branched alkane	$C_{19}H_{40}$	268.5	21.034	2405844	66078.7	0.58
Cyclobutanol	Cycloalkanol	C_4H_8O	72.11	21.264	882509	28317.4	0.25
1,3-Propanediamine, N-methyl-	Diamine	$C_4H_{12}N_2$	88.15	21.555	1007972	29536.6	0.26
d-Mannitol, 1-decylsulfonyl-	Sugar alcohol with sulfur	$C_{16}H_{34}O_7S$	370.5	21.740	892217	32067.3	0.28
2-Propenamide	Amide	C_3H_5NO	71.0779	21.815	1165515	30380.1	0.26
2-Trifluoroacetoxypentadecane	Fluro compound	$C_{17}H_{31}F_3O_2$	324.4	22.020	967350	35501.8	0.31

Dodecane, 2-methyl-	Isomer of tridecane	$C_{13}H_{28}$	184.36	22.290	1316547	54282.4	0.48
Hexadecane, 1-chloro-	Alkyl halide	$C_{16}H_{33}Cl$	260.9	22.395	938053	30785.4	0.27
Heptacosane	Alkane	$C_{27}H_{56}$	380.7	22.445	2577712	95117.9	0.84
Cyclopropane, pentyl-	Cycloalkane	C_8H_{16}	112.21	22.485	1591303	48871.3	0.43
Palmitic acid (Hexadecanoic acid)	Saturated fatty acid	$C_{16}H_{32}O_2$	256.42	23.055	11037976	542378.1	4.79
Butanal, 3-hydroxy-	Aldehyde	$C_4H_8O_2$	88.11	23.630	1166267	40663.4	0.35
Pentadecanal-	Fatty aldehyde	$C_{15}H_{30}O$	226.40	23.941	2381514	98228.4	0.86
Octadecane, 3-ethyl-5-(2-ethylbutyl)-	Alkane	$C_{26}H_{54}$	366.7	24.296	912906	28138.3	0.24
Stearyl alcohol	Saturated fatty alcohol	$C_{18}H_{38}O$	270.5	24.856	1898116	92123	0.81
1-Iodo-2-methylundecane	Iodoalkane	$C_{12}H_{25}I$	296.23	25.391	1524788	93294.3	0.82
Cyclohexane, 1,1'-(2-ethyl-1,3-propanediyl)bis-	Cycloalkane	$C_{17}H_{32}$	236.4	25.611	1840989	62965.8	0.55
Octadecanoic acid (Stearic acid)	Saturated fatty acid	$C_{18}H_{36}O_2$	284.4772	26.001	5501762	290697.9	2.56
Ursolic acid	Pentacyclic triterpenoid	$C_{30}H_{48}O_3$	456.7	26.096	1100460	33725.9	0.29
4,6-di-tert-Butylresorcinol	Phenol	$C_{14}H_{22}O_2$	222.32	26.156	1287866	34707.9	0.30
Sinapic acid	Phenolic acid	$C_{11}H_{12}O_5$	224.21	26.602	857163	29084.8	0.25
Benzenemethanol, à-(1-aminoethyl)-	Aromatic alcohol and an amine	$C_9H_{13}NO$	151.205	28.487	1418980	44405.4	0.39
Octadecane, 1,1'-[1,3-propanediylbis(oxy)]bis-	Alkane ether	$C_{39}H_{80}O_2$	581.1	28.552	816978	30703.4	0.27
6-Fluoro-5-(4-methylpiperazin-1-yl)benzo[1,2, 5]oxadiazol-1-oxide	Oxadiazole	$C_{11}H_{13}FN_4O_2$	252.24	28.712	1119916	53106.8	0.46
1,3,5-Triazine-2,4-diamine, 6-bromo-N,N'-diethyl-	Nitrogen-containing compound	$C_7H_{12}BrN_5$	246.11	28.943	1209151	31835.6	0.21
2-Hexanamine, 4-methyl-	Primary amine	$C_7H_{17}N$	115.216	29.133	1513065	35112	0.31
Penoxaline	Aniline	$C_{13}H_{19}N_3O_4$	281.31	29.883	1164598	32055.3	0.28
1-(2-Acetoxyethyl)-3,6-diazahomoadamantan-9-one oxime	Oxime	$C_{13}H_{21}N_3O_3$	267.32	31.694	1269057	28682.8	0.25
Carbamic acid, N-[10,11-dihydro-5-(2-methylamino-1-oxoethyl)-3-5H-dibenzo[b, f]azepinyl]-, ethyl ester	Carbamate ester	$C_{20}H_{23}N_3O_3$	353.4	32.394	1147641	28319.3	0.25
2-Butanone, (2,4-dinitrophenyl) hydrazone	Ketone with hydrazine derivative	$C_{10}H_{12}N_4O_4$	252.23	33.404	882237	48628	0.43

Treatment with HPE alleviates the dysfunctionality of the liver and kidney functions

Our results showed that there was a highly significant increase ($p < 0.05$) in ALT and AST activities, and total bilirubin concentrations while significant decrease in albumin in CTX injected group when compared with control group. Additionally, CTX/ HPE group showed a significant decrease ($p < 0.05$) in ALT and AST activities, and total bilirubin while not significant change in albumin concentration when compared with CTX-group. The treatment with HPE-group did not reveal any significant changes ($p> 0.05$) in the uric acid and creatinine concentrations when compared with control group. However, the results from CTX-group showed extremely significant increase ($p< 0.05$) in uric acid and creatinine

levels if compared with control group. CTX/HPE group showed significant decreases in the uric acid and creatinine levels ($p< 0.05$) when compared to the CTX- group as shown in (Table 2).

Treatment with HPE ameliorates serum electrolytes levels post CTX-injection

The results showed that highly significant increase ($p< 0.05$) in electrolytes levels (Na^+, K^+, Ca^{2+}, Cl^-, and Mg^{2+}) in CTX-group when compared with control group. However, CTX/HPE group showed a significant decrease in all electrolyte levels ($p< 0.05$), except Mg, when compared to the CTX-group as shown in (Table 3).

Table 2. Effects of treatments on liver and kidney function tests of all experimental groups.

Groups	ALT (U/L)	AST (U/L)	Albumin (mg/dL)	T. Bil (mg/dL)	Create (mg/dL)	Uric acid (mg/dL)
Ctrl.	33.83 ± 0.76 [c]	42.57 ± 0.51 [c]	3.68 ± 0.15 [a]	0.55 ± 0.03 [d]	0.7 ± 0.03 [b]	2.5 ± 0.1 [c]
HPE	31.43 ± 0.4[d]	43.27 ± 1.1 [c]	3.31 ± 0.11 [a]	0.65 ± 0.04 [c]	0.54 ± 0.04 [b]	2.9 ± 0.16 [c]
CTX	47.6 ± 0.53 [a]	60.53 ± 0.5 [a]	2.66 ± 0.21 [b]	0.94 ± 0.04 [a]	1.21 ± 0.25 [a]	3.33 ± 0.25 [a]
CTX/HPE	39.13 ± 0.23 [b]	52.57 ± 0.51 [b]	2.86 ± 0.05 [b]	0.75 ± 0.04 [b]	0.8 ± 0.02 [b]	3.02 ± 0.1 [b]
p-value	< 0.001	< 0.001	< 0.001	< 0.001	0.001	0.001

The data presented as mean ± SD at ($p< 0.05$). Superscript letters (a, b, c, and d) represented that groups with different letters indicate statistically significant differences. Ctrl: Control, HPE: *Holothuria polii*-extract, CTX: Cyclophosphamide, CTX/HPE: Cyclophosphamide and *Holothuria polii*-extract, ALT: Alanine aminotransferases, AST: Aspartate aminotransferases, T. Bil: Total bilirubin

Table 3. Effects of treatments on serum electrolyte levels of all experimental groups

Group	Na (mmol/L)	K (mmol/L)	Ca (mg / dL)	Cl (mmol/L)	Mg (mg / dL)
Ctrl.	123.66 ± 0.57 [c]	3.27 ± 0.15 [c]	5.6 ± 0.2 [d]	98.47 ± 0.45 [c]	1.71 ± 0.15 [c]
HPE	121.44 ± 0.51 [d]	3.58 ± 0.1 [c]	6.47 ± 0.31 [c]	95.87 ± 0.45 [d]	1.91 ± 0.02 [b, c]
CTX	147.11 ± 0.2 [a]	5.27 ± 0.21 [a]	9.47 ± 0.06 [a]	112.33 ± 0.58 [a]	2.37 ± 0.07 [a]
CTX/HPE	138.63 ± 0.55 [b]	4.11 ± 0.17 [b]	7.7 ± 0.26 [b]	104.56 ± 0.51 [b]	2.16 ± 0.14 [a, b]
p-value	0.000	0.000	0.000	0.000	0.000

The data presented as mean ± SD. Superscript letters (a, b, c, and d) represented that groups with different letters indicate statistically significant differences. Ctrl: Control, HPE: *Holothuria polii*-extract, CTX: Cyclophosphamide, CTX/HPE: Cyclophosphamide and *Holothuria polii*-extract, Na: Sodium, K: Potassium, Ca: Calcium, Cl: Chloride, Mg: Magnesium.

Treatment with HPE ameliorates post CTX-injection augmented the antioxidant parameters

The data obtained from CTX-injected group (Gp3) showed a highly significant decrease ($p< 0.05$) in the levels of the antioxidant parameters (SOD, CAT and GSH levels) when compared with the control group. Additionally, there was a highly significant increase in MDA level in CTX-injected group when compared with the control group. However, CTX/HPE group showed a highly significant increase in the antioxidant parameters and an incredible significant decrease in MDA level ($p< 0.05$) when compared to the CTX-group, suggesting a protective effect of HPE against CTX-induced oxidative damage as shown in (Fig. 2).

Treatment with HPE alleviating CTX effect on pro-inflammatory cytokines and apoptotic marker

The results demonstrated a significantly substantial rise in pro-inflammatory cytokine levels (TNF-α and IL-1β) in rats group injected with CTX compared to the control group, indicating strong inflammatory response induced by CTX. The data obtained from this study revealed a highly significant increase ($p < 0.05$) in apoptotic marker (caspase-3) levels in the CTX-injected group when compared with control group, suggesting a strong apoptotic response due to CTX. However, CTX/HPE group showed an incredible significant decrease in the pro-inflammatory cytokines and apoptotic marker level ($p< 0.05$) when compared to the CTX-group, indicating that treatment with HPE alleviated CTX inflammatory effect and reduced apoptosis but it did not restore the value to the control levels as shown in (Fig. 3).

Treatment with HPE post CTX-injection improves angiotensinogen, angiotensin-II, renin and aldosterone

The data obtained from (Fig. 4) showed that the concentrations of angiotensinogen, angiotensin-II, renin, and aldosterone revealed non-significant alternations ($p> 0.05$) in HPE-group when compared with control group. The results showed that there was highly significant increase ($p< 0.05$) in angiotensinogen, angiotensin-II, renin and aldosterone concentrations in CTX-injected group when compared with the control group. Additionally, CTX/HPE group demonstrated a significant decline ($p< 0.05$) in angiotensinogen, angiotensin-II, renin, and aldosterone concentrations when compared with CTX-injected group.

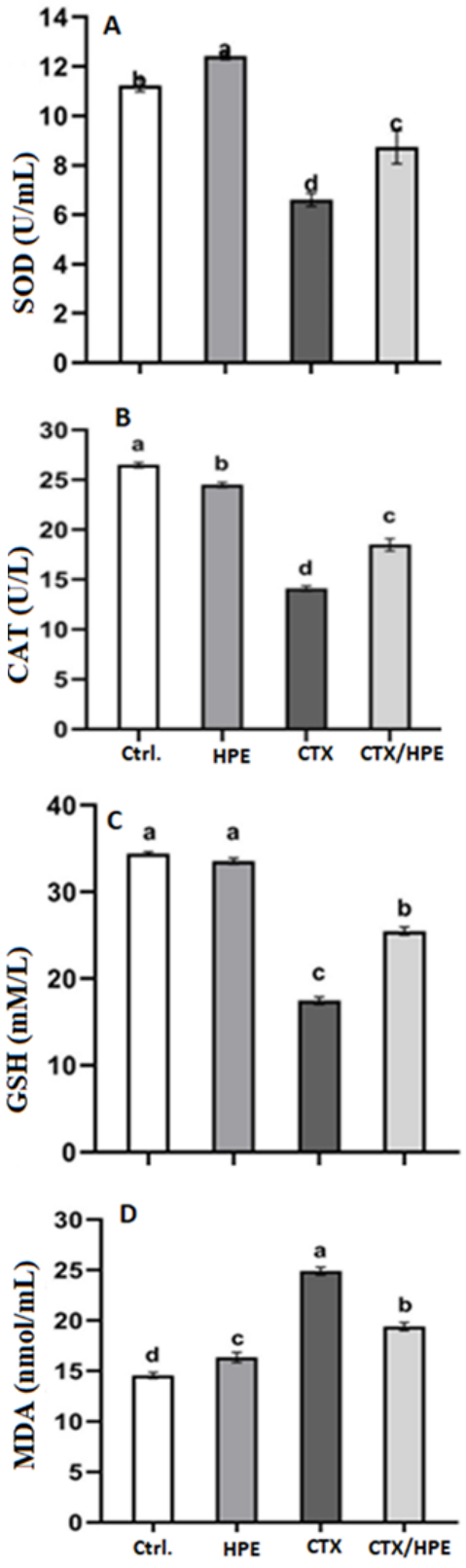

Fig. 2. SOD, CAT activities, GSH and MDA levels in different rat groups. Ctrl: control, HPE: *Holothuria polii*-extract, CTX: cyclophosphamide, CTX/HPE: cyclophosphamide and *Holothuria polii*-extract

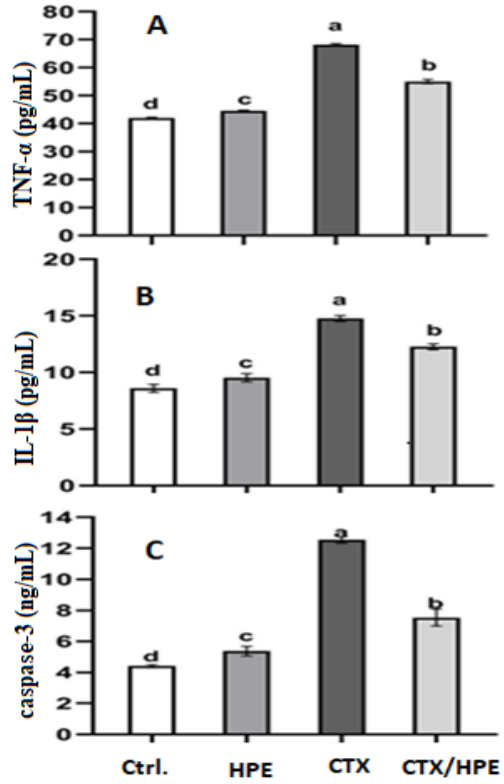

Fig. 3. The levels of A- TNF-alpha, B- IL-1β and C- caspase-3 in different rat groups under the study. Ctrl: control, HPE: *Holothuria polii*-extract, CTX: cyclophosphamide, CTX/HPE: cyclophosphamide and *Holothuria polii*-extract

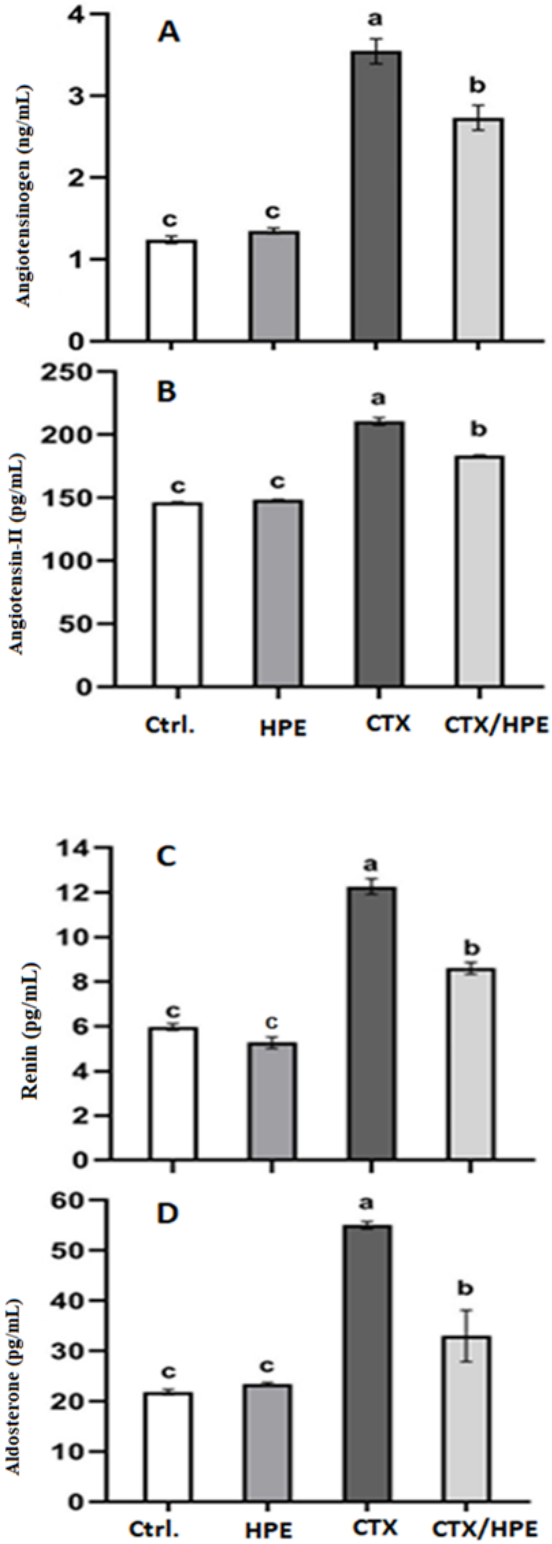

Fig. 4. The levels of angiotensinogen, angiotensin-II, renin, and aldosterone in different rat groups. Ctrl: control, HPE: *Holothuria polii*-extract, CTX: cyclophosphamide, CTX/HPE: cyclophosphamide and *Holothuria polii*-extract.

Treatment with HPE post-CTX injection ameliorates the histopathological changes in the liver, kidney and lung tissues

Microscopic examination of liver sections of control and HPE-group groups stained with hematoxylin and eosin revealed normal liver architecture, including central vein, hepatocytes, and blood sinusoid with Kupffer cells (Fig. 5 A and B). On the opposite side, the CTX-injected group exhibited the liver loss of regular architecture, including congested central vein, degenerated hepatocytes with necrotic nuclei, leukocyte infiltration, and blood sinusoid with hemorrhage (Fig. 5 C). The liver sections in rats treated with CTX/HPE showed a marked degree of improvement in liver architecture if compared to CTX-injected group, but with limited hemorrhage blood sinusoid still present (Fig. 5 D).

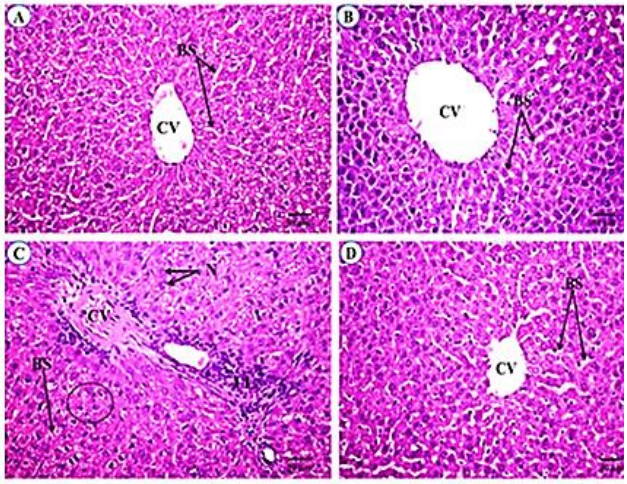

Fig. 5. Photomicrographs of liver sections of all experimental groups. control (A) and HPE (B) groups, exhibited normal liver architecture, including central vein (CV), hepatocytes (HC), and blood sinusoid (BS) with Kupffer cells. CTX-injected group (C) exhibited congested central vein (CV), degenerated hepatocytes (black circle) with necrotic nuclei (N), leukocyte infiltration (LI), and blood sinusoid (BS) with hemorrhage. CTX/HPE group (D) showed normal liver architecture, similar to the control, but with limited hemorrhage blood sinusoid (BS) still present. (H&E, X400).

Histological examination of kidney sections of control and HPE-group groups stained with hematoxylin and eosin exhibited normal kidney architecture, including normal glomerular capsule, glomerulus and normal tubule histological structure (Fig. 6 A and B). On the opposite side, the CTX-injected group exhibited the kidney loss of regular architecture, including glomerular atrophy, tubule degeneration with necrotic nuclei, and blood vessel congestion and dilatation (Fig. 6 C). Rats treated with CTX/HPE showed normal kidney architecture, similar to the control, but with limited glomerular atrophy still present (Fig. 6 D).

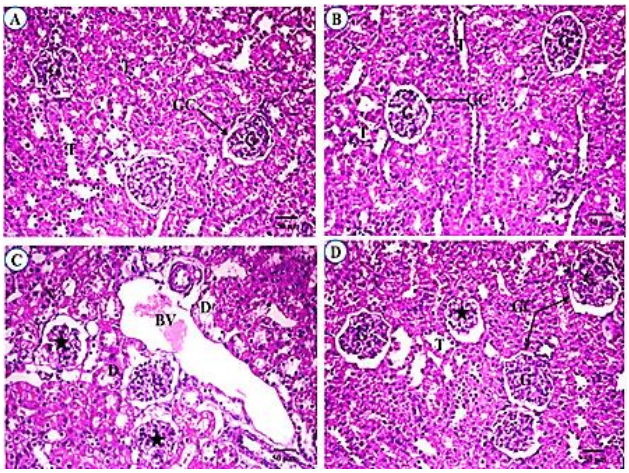

Fig. 6. Photomicrographs of kidney sections of all experimental groups. Control (A) and HPE (B) groups, showed normal kidney architecture, including glomerular capsule (GC), glomerulus (G) and normal tubule histological structure (T). CTX-injected group (C) exhibited glomerular atrophy (black star), tubule degeneration (D) with necrotic nuclei, and blood vessel (BV) congestion and dilatation. CTX/HPE group (D) showed normal kidney architecture, similar to the control, but with limited glomerular atrophy (black star) still present. (H&E, X400).

As shown in (Figure 7 A and B) which represented the control and HPE-alone, the results showed that these groups exhibit normal pulmonary parenchyma, including normal alveolar septa and normal pneumocytes histological structure. On the opposite side, the CTX-injected group exhibits complete obstruction of the alveoli with thickened alveolar septa, severe edema in the interalveolar septa, and leukocyte infiltration of inflammatory cells (Fig. 7 C). Rats treated with CTX/HPE group demonstrated mild improvement in lung architecture, near to the control, while their alveolar septa remained thickened (Fig. 7 C).

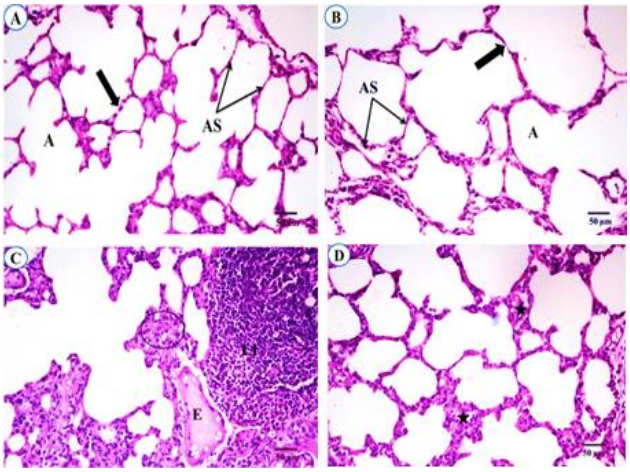

Fig.7. Photomicrographs of lung sections of all experimental groups. Control (A) and HPE (B) groups, exhibited normal pulmonary parenchyma, including normal alveoli (A) with alveolar septa (AS) and normal pneumocytes histological structure (thick arrow). CTX-injected group (C) exhibited complete obstruction of the alveoli with thickened alveolar septa (black circle), severe edema (E) in the inter-alveolar septa, and leukocytes infiltration of inflammatory cells (II). CTX/HPE group (D) showed mild restoration of lung architecture, near to the control with still thickened alveolar septa (black star). (H&E, X400).

4. Discussion

CTX is a key component of numerous chemotherapeutic protocols, demonstrating broad-spectrum efficacy against various malignancies and non-cancerous conditions and its use has been associated with several side effects (Srirangan and Sabina, 2025). This study showed that HPE ameliorates CTX induced injuries in liver, kidney and lung tissues in experimental rats. In the present study, *H. polii* crude extract presented different chemical constituents at different retention times. Palmitic acid was the most abundant compound in *H. polii* crude extract, followed by octadecanoic acid, 2-bromo dodecane, and hexadecane with peak areas of 4.793, 2.569, 1.869, and 1.089%, respectively. These bioactive compounds have different biological activities. Palmitic acid is saturated fatty acid having antioxidants and anti-inflammatory properties (Subavathy and Thilaga, 2016). It can also reduce pulmonary edema and respiratory failure (Babu et al., 2014). Moreover, hexadecane, myristic acid, and sinapic acid are known to exhibit antioxidant and anti-inflammatory activities (Arora and Kumar, 2018). Dodecane, 5,8-diethyl can provide protection against pulmonary edema and muscle weakness (Babu et al., 2014). Remarkably, sinapic acid can attenuate high blood pressure, myocardial and vascular dysfunction, cardiac fibrosis, oxidative stress, and angiotensin-converting enzyme activity (Silambarasan et al., 2014).

Ursolic acid is a pentacyclic triterpenoid with a variety of potential health benefits, including anti-inflammatory and antioxidant properties (Zhao et al., 2019). Sundaresan et al. (2012) documented that oral administration of ursolic acid alone markedly decreased blood pressure in C57BL/6J mice subjected to a high-fat diet. An intragastric administration of 50 mg/kg of ursolic acid markedly decreases systolic and diastolic blood pressure without influencing heart rate in male spontaneous hypertensive Wistar rats (Flores-Flores et al., 2016). Oyagbemi et al. (2016) demonstrated that antioxidants could shield healthy cells from the harmful effects of CTX.

The findings of this study indicated significant increase in the activities of ALT, AST, as well as total bilirubin, creatinine and uric acid levels by CTX. Moreover, there was a significant decrease in the levels of albumin in the test group administered CTX relative to the control group. These findings were confirmed by Agbara et al. (2024) and Alshater et al. (2021) similarly reported a substantial elevation in serum liver and kidney marker after to the induction of hepato-renal toxicity by CTX. Furthermore, the elevated total bilirubin in the CTX-group is consistent with established pathways for liver damage and cholestasis brought on by CTX (Ahmed et al., 2019). According to earlier research, Kumar et al. (2022) revealed that CTX is extensively metabolized in the liver by Cytochrome p-450 into its active metabolites, which include 4-hydroxy-CTX, phosphoramide mustard, and acrolein. The 4-hydroxy-CTX is converted by the liver into phosphoramide mustard, which alkylates purine base cross-linking in DNA and prevents the production of DNA, RNA, and proteins. This results in the death of rapidly dividing cells. The direct toxic impact of CTX and its metabolites induces changes in cell membrane integrity via lipid peroxidation, leading to liver damage. Its metabolites also

cause liver tissue harm, manifesting as sinusoidal obstruction syndrome, characterized by hepatic necrosis and blockage of hepatic venous flow. Sinusoidal obstruction syndrome manifested as abrupt abdominal pain, weight gain, and ascites, later presenting as jaundice and hepatic impairment. According to earlier research, many invertebrate extracts such as ink extract and polysaccharide of *Sepia officinalis* have cytoprotective and antioxidant qualities that lessen the oxidative damage caused by CTX (Alshater et al 2021). The treatment with *Phoenix dactylifera* seeds extract showed significantly ameliorated the hematological, biochemical, and histological alterations post CTX injection as evidenced by improving the liver/kidney functions (El-Naggar et al., 2023). This is supported by the hepatoprotective impact of HPE seen here, especially in the CTX/HPE group.

The current study evaluated the effects of CTX, HPE, and co-treatment CTX with HPE on serum electrolyte levels and found that the concentrations of Na^+, K^+, Ca^{2+}, Cl^-, and Mg^{2+} changed significantly. The equilibrium of electrolytes is crucial for sustaining homeostasis within the body. The primary electrolytes are Na+, K+, Mg2+, Cl-, and Ca2+. These ions regulate bodily fluid volume and blood pressure, facilitate muscle contractions and nerve conduction, and play a crucial role in enzymatic activities. The kidneys primarily maintain balance by regulating urine volume and composition, facilitating the excretion of excess electrolytes (Gałęska et al., 2022). When compared to the control group, serum levels of Na, K, Ca, Cl, and Mg were significantly higher after CTX therapy alone. According to Zhang et al. (2015), these findings are consistent with earlier research that found that administering CTX was linked to electrolyte abnormalities, including hypernatremia, hyperkalemia, and hypercalcemia. These abnormalities were most likely caused by renal tubular damage and changed membrane permeability. It is known that CTX causes oxidative stress, which impairs kidney function and upsets electrolyte balance (Shalaby et al., 2016). In contrast to the control group, the HPE-group showed higher levels of Ca and lower levels of Na and Cl. Antioxidants are essential for preserving electrolyte balance in biological systems by alleviating oxidative stress, which can interfere with cellular functions dependent on electrolytes. They achieve this by neutralizing free radicals, safeguarding cellular components from damage, and facilitating the operation of electrolyte pumps and channels. This shows that HPE may stabilize electrolyte homeostasis, perhaps as a result of its antioxidant and renal-protective qualities. It's interesting to note that the CTX and HPE group showed intermediate values and electrolyte disturbances were lessened in comparison to the CTX-alone group.

As seen by elevated MDA and decreased SOD, CAT, and GSH, the CTX therapy markedly increases oxidative stress. These results are consistent with earlier studies that showed that administering CTX caused oxidative damage *via* reactive oxygen species (ROS) and weakened the antioxidant defenses (El-Sheikh et al., 2020). The substantial decrease in SOD and CAT activities after CTX administration is in line with research by Li et al. (2019), who found that CTX increases cellular vulnerability to oxidative damage by upsetting the enzymatic antioxidant balance. Additionally, the decrease in GSH levels seen in the CTX group confirms previous research by Abdel-Daim and Ghazy (2015), which showed that GSH depletion is a defining feature of toxicity caused by CTX. Remarkably, co-administration of HPE and CTX resulted in a decrease in MDA levels and a partial recovery of antioxidant indicators. This implies that HPE has antioxidative qualities that can lessen oxidative damage brought on by CTX. Numerous plants extract high in polyphenols and flavonoids, which are known to scavenge free radicals and strengthen endogenous antioxidant systems, have been shown to exhibit these protective benefits (Saeed et al., 2017). HPE's protective function against CTX-induced oxidative stress is consistent with research showing that natural substances such thymoquinone, resveratrol, and curcumin successfully reduce oxidative damage brought on by chemotherapy (Ghosh et al., 2020). These substances usually maintain cellular integrity by lowering lipid peroxidation and

increasing antioxidant enzymes. The current research supports the theory that combining natural antioxidants with chemotherapy drugs such as CTX may be a viable way to reduce adverse effects associated with oxidative stress, hence enhancing patient safety and therapeutic results. According to the current investigation, CTX considerably increased the levels of the apoptotic marker caspase-3 and the inflammatory cytokines TNF-α and IL-1β when compared to control groups. These results are in line with earlier research showing that CTX causes inflammation and oxidative stress, which further damages tissue by triggering pro-inflammatory pathways (El-Sayyad et al., 2021). The recruitment of immune cells and the enhancement of apoptotic signaling are two key mediators of CTX-induced toxicity, specifically TNF-α and IL-1β (Olayoku et al., 2020). The notable increase in these cytokines seen in the CTX-group is consistent with earlier research that found CTX increases nuclear factor-kappa B (NF-κB) signaling pathways, which in turn exacerbates systemic inflammation (Cao et al., 2018).

Oxidative stress induces NF-κB to become activated in tissues treated with CTX, which leads to tissue damage by producing cytokines that promote inflammation, like TNF-α and IL-6 (Caglayan et al., 2018). Outcomes of the investigation showed that CTX exposure is boosting the gene expression of caspase-3. A highly active cysteine protease in the caspase family, caspase-3 is essential for both intrinsic and extrinsic apoptotic processes. One reliable indicator of cellular apoptosis is caspase-3 (Khalilzadeh et al., 2017). Significant rise in caspase-3 levels further emphasizes CTX's function in triggering apoptosis, a process that has been connected to its cytotoxic effects in a number of tissues, including the kidneys, liver, and immunological organs (Shah et al., 2017). Remarkably, when compared to CTX-alone treatment, co-treatment with HPE significantly decreased TNF-α, IL-1β, and caspase-3 levels, indicating a protective function. This is consistent with previous research that demonstrated that plant-derived extracts high in antioxidants and polyphenols could reduce oxidative and inflammatory damage brought on by CTX (Alqahtani et al., 2020). According to Ijaz et al. (2022), herbacetin may be a viable protective drug against CTX-induced nephrotoxicity and renal histological damage; this protection may be brought about by the compound's anti-inflammatory, anti-apoptotic, and antioxidant properties. Moreover, the slight but statistically significant increase in inflammatory markers following HPE treatment, compared to control, may reflect mild immune activation, which has been reported with certain bioactive plant components (Lee et al., 2016). Nonetheless, the levels remained substantially lower than those observed in the CTX-group, underscoring the net protective impact when used in combination therapy. Collectively, the data suggests that HPE co-administration may offer a promising adjunctive strategy to ameliorate CTX-induced inflammatory and apoptotic damage, thereby enhancing the safety profile of chemotherapy regimens.

Confirming earlier findings, CTX treatment markedly increased renin-angiotensin system components (ROS), including angiotensinogen, angiotensin II, renin, and aldosterone, as a result of CTX-induced oxidative stress, tissue damage, and inflammation due to generation of ROS (Wang et al., 2019). A common way to describe the process is as an enzymatic cascade that starts with the breakdown of angiotensinogen in the liver and ends with the production of angiotensin I by circulating renin, which is released by the juxtaglomerular apparatus of the kidney. In the pulmonary capillaries, angiotensin converting enzyme produces angiotensin II, the principal effector peptide of the system. Angiotensin II plays a role in inflammation and wound healing by releasing critical cytokines and producing extracellular matrix. Angiotensinogen, a big protein of 485 amino acids that includes a 33-amino-acid signal peptide and a 10-amino-acid N-terminus, is synthesized in the liver at the start of all RAS pathways. Surprisingly, angiotensinogen production is elevated in liver dysfunction and affects hepatic stellate cells, even when other protein synthesis is reduced globally. Since activated hepatic stellate cells release additional angiotensinogen, this seems

to constitute a positive feedback loop (McGrath and Wentworth, 2024). In line with research on antioxidant-rich natural extracts, HPE treatment had no effect and preserved RAS stability (Park et al., 2020). Crucially, when compared to CTX alone, CTX and HPE co-treatment reduced levels of all evaluated indicators and partially reversed CTX-induced RAS activation, confirming the protective function of extracts rich in polyphenols and flavonoids against nephrotoxic damage (El-Sayed et al., 2020). These results are consistent with past studies on natural substances that restore RAS function and imply that HPE may provide anti-inflammatory and antioxidant defenses against CTX toxicity (Zhang et al., 2018).

The post-treatment with HPE ameliorated the hepatic, renal, and lung dysfunctions and decreases the histological changes which were induced by CTX The histopathological results obtained from CTX group showed that highly damage in the liver architecture through congested central vein, degenerated hepatocytes with necrotic nuclei, leukocyte infiltration of inflammatory cells, and blood sinusoid with hemorrhage. The present findings were confirmed by Abdel-Wahhab et al. (2021), who illustrated that CTX damages the liver by infiltrating leukocytes, causing severe inflammation, and necrotic hepatocytes. These pathological alterations showed a strong correlation with the changed enzyme activity, and another earlier investigation confirmed similar results (Lixin et al., 2019). Accordingly, CTX can change the antioxidant defense system and detoxification state by causing oxidative stress and liver damage. Low dose of CTX (200 mg/kg) might cause hepatotoxicity (Oyagbemi, et al., 2016). CTX has been demonstrated to elevate ROS production and induce DNA damage in the livers of rats (Aladaileh et al., 2019). The biochemical values were also supported by histopathological investigations.

The histopathological results obtained from CTX treated rats showed that high damage in the kidney architecture through glomerular atrophy, tubule degeneration with necrotic nuclei, and blood vessel congestion and dilatation. The results were confirmed by Alshahrani et al. (2022) who showed that histopathological findings reveal that CTX-induced renal injury, characterized by inflammatory cell infiltration and significant changes in renal architecture, is linked to free radical-induced oxidative stress, and extensive renal impairments. CTX, a drug causing renal toxicity, causing increased free radical generation, oxidative stress, and kidney cell damage, leading to CTX-induced nephrotoxicity is reported to be mediated through oxidative stress (Ayza et al., 2022). Similar results confirmed that, the kidneys of mice given CTX, there was a degradation of tubular architecture, congestion, edema, and necrosis, along with peritubular and glomerular congestion, desquamation of epithelial cells, and inflammatory cell invasion (Rehman et al., 2012). The histopathological findings from CTX treated rats indicated that treatment with CTX induced damage to lungs and total alveolar obstruction accompanied by thickened alveolar septa, significant edema in the interalveolar septa, and leukocyte infiltration of inflammatory cells, potentially resulting from CTX-induced major cellular changes, including elevated ROS production and lipid peroxidation add in lung tissue.

Accordingly previous studies have demonstrated histopathological analyses of CTX-intoxicated rats revealed total alveolar blockage, thicker inter-alveolar septa, expanded blood vessels, and pronounced inflammatory edema accompanied by pyknotic nuclei (Saghir et al., 2020). Similarly, Hassanein et al. (2023) demonstrated that a single CTX injection at a dosage of 200 mg/kg led to considerable pulmonary and cardiac toxicity. In the lungs, CTX induces pulmonary damage characterized by congestion, edema, bleeding with inflammatory infiltration, and constricted alveoli with thickened septa. Identical results were noted in earlier research (Saghir et al., 2020; Şengul et al., 2017). Reduced levels of antioxidant enzymes and lipids and proteins are two ways in which ROS harm cells. ROS cause lipid peroxidation, which can compromise cell membrane integrity and ultimately lead to cell death (Amirkhizi et al., 2010). Lipid peroxidation may enhance the role of ROS through

branched chain reactions, and the concentration of lipid peroxides might indicate the extent of cellular damage. Besides lipid peroxidation, ROS can oxidize cellular proteins and degrade DNA. MDA levels were considerably elevated in the lungs of CTX treated rats, indicating lipid and protein damage, respectively.

In Conclusion, the current studies indicated that HPE alleviated CTX-induced electrolyte imbalances and improved both physiological functions and histological structure of liver, kidney, and lung in CTX treated rats through its antioxidant and anti-inflammatory activities.

5. Reference

Abdel-Daim MM, Ghazy EW, 2015. Effects of diethyl phthalate on oxidative stress markers, cytogenetic parameters, and hepatic histopathology in rats: The protective role of alpha-lipoic acid. Environ Sci Pollut Res Int, 22: 11568-11574.

Abdel-Wahhab KG, Mannaa FA, Ashry M, Khaled DM, Hassan LK, Gomaa HF, 2021. *Chenopodium quinoa* ethanolic extract ameliorates cyclophosphamide®-induced hepatotoxicity in male rats. Comp. Clin. Pathol. 30: 267-276.

Agbara AC, Ajah MP, Offor CE, Anyaoku CI, Erhabor OD, Nwobodo VO, 2024. Effect of *Cucumeropsis manni* Seed Oil on Liver and Kidney Function Markers of Cyclophosphamide Induced Toxicity in Wistar Albino Rats. ANACHEM Journal, 15(1), 154-167.

Ahmed OM, Abd El-Tawab SM, Ahmed RG , 2019. Effects of cyclophosphamide on oxidative stress and hepatic injury markers: Role of antioxidants. Biomed. Pharmacother.111, 760-770

Aladaileh SH, Abukhalil MH, Saghir SA., Hanieh H, Alfwuaires MA, Almaiman AA, Bin-Jumah M, Mahmoud AM, 2019. Galangin activates nrf2 signaling and attenuates oxidative damage, inflammation, and apoptosis in a rat model of cyclophosphamide-induced hepatotoxicity. Biomolecules 2019, 9, 346.

Alqahtani A, Alshammari G, Alharbi M, Alhazzani K, 2020. Protective effect of plant extracts against cyclophosphamide-induced organ toxicity: A review. Pharm. Biol. 58: 358–366.

Alsemeh AE, Abdullah DM, 2022. Protective effect of alogliptin against cyclophosphamide-induced lung toxicity in rats: Impact on PI3K/Akt/FoxO1 pathway and downstream inflammatory cascades. Cell Tissue Res. 388: 417-438.

Alshahrani S, Ali Thubab H M, Ali Zaeri AM, Anwer T, Ahmed RA, Jali AM, Alam MF, 2022. The protective effects of sesamin against cyclophosphamide-induced nephrotoxicity through modulation of oxidative stress, inflammatory-cytokines and apoptosis in rats. Int. J. Mol. Sci. 23: 11615.

Alshater AA, Ali RA, Dakhly HF, 2021. Ameliorative effect of ink extract and polysaccharide of Sepia officinalis on hepatotoxicity, renal toxicity and hematological disorders in adult male albino rats treated with cyclophosphamide. SVU-Int. J. Agric. Sci, 3:108-121.

Amirkhizi F, Siassi F, Minaie S, Djalali M, Rahimi A, Chamari M, 2010. Is obesity associated with increased plasma lipid peroxidation and oxidative stress in women? ARYA Atheroscler. J. 2(4): 20.

Arora S, Kumar G, 2018. Phytochemical screening of root, stem and leaves of Cenchrus biflorus Roxb. J Pharmacogn. Phytochem. 7(1), 1445-1450.

Ayza MA, Zewdie KA, Yigzaw EF, Ayele SG, Tesfaye BA, Tafere GG, Abrha MG, 2022. Potential Protective Effects of Antioxidants against Cyclophosphamide-Induced Nephrotoxicity. Int. J. Nephrol. 1: 5096825.

Babu M, Raja DP, Arockiaraj AA, Vinnarasi J, 2014. Chemical constituents and their biological activity of *Ulva lactuca* Linn. Int. J. Pharm. Drug Anal, 2(7): 595-560.

Boopathi E, Thangavel C, 2021. Dark side of cancer therapy: Cancer treatment-induced cardiopulmonary inflammation, fibrosis, and immune modulation. Int. J. Mol. Sci. 22(18): 10126.

Brandi G, Frega G, 2019. Microbiota: overview and implication in immunotherapy-based cancer treatments. Int. J. Mol. Sci.20(11), 2699.

Caglayan C, Temel Y, Kandemir FM, Yildirim S, Kucukler S, 2018. Naringin protects against cyclophosphamide-induced hepatotoxicity and nephrotoxicity through modulation of oxidative stress, inflammation, apoptosis,

autophagy, and DNA damage. Environ. Sci. Pollut. Res. 25: 20968-20984.

Cao L, Chen J, Su J, Zhao J, 2018. Cyclophosphamide-induced nephrotoxicity: The protective role of natural products. Environ. Toxicol. Pharmacol. 62: 61-67.

Cao L, Du J, Nie Z, Jia R, Yin G, Xu P, Xu G, 2022. Alteration of endoplasmic reticulum stress, inflammation and anti-oxidative status in cyclophosphamide-damaged liver of Nile tilapia (*Oreochromis niloticus*). Comp. Biochem. Physiol. C.Toxicol. Pharma col. 254: 109271.

Delle Chiaje S, 1823. Memorie sulla storia e notomia degli animali senza vertebre del regno di Napoli. Dalla Stamperia Società Tipografica de'Fratelli Fernandes, Napoli 4:184 pp.

Drury RA, Wallington EA, 1980. Preparation and fixation of tissues. In: RAB D, Wallington EA (eds) Carleton's histological technique. 5. Oxford University Press, Oxford, pp 41–54.

Elbandy M, 2022. Anti-inflammatory effects of marine bioactive compounds and their potential as functional food ingredients in the prevention and treatment of neuroinflammatory disorders. Molecules. 28(1), 2.

El-Naggar SA, Abdel-Farid IB, Germoush MO, Elgebaly HA, Alm-Eldeen AA, 2016. Efficacy of *Rosmarinus officinalis* leaves extract against cyclophosphamide-induced hepatotoxicity. Pharm. Biol. 54(10): 2007-2016.

El-Naggar SA, Basyouny MA., Amin SE, Elwan, M, 2023. *Phoenix dactylifera* seeds extract ameliorates the hepato-renal toxicities that induced by cyclophosphamide in male mice. Biol. Biomed. J. 1(1): 1-10.

El-Saidy SA, El-Feki AS, El-Khodary GM, Hassan AA, Elgendy DI, Gawaan YM, 2024. A potential therapeutic effect of sea cucumber *Holothuria polii* extract during the intestinal phase of experimental trichinellosis. Journal of Parasitic Diseases: 1-18.

El-Sayed WM, Al-Kahtani MA, Abdel-Moneim AM, 2020. Role of antioxidants in prevention of cyclophosphamide-induced organ toxicity: A review. Pharmacol. Res. 152:104600.

El-Sayed YA, Abdel-Moneim AE, Taha RG, Khalil MF, Abdel-Gaber R, Thagfan FA, Dkhil MA, 2024. *Holothuria polii* extract as a potential anticoccidial agent: Evidence of its MUC2 regulatory impact in murine jejunum. Vet. Sci. 11(10): 490.

El-Sayyad HI, Ismail MF, Shalaby FM, Abou-El-Magd RF, Gaur RL, Fernando A, Raj, MH, 2021. Protective mechanisms of antioxidantts against cyclophosphamide-induced cytotoxicity: An updated review. Curr. Pharm. Biotechnol, 22:1390–1400.

El-Sheikh MA, Alkahtani S, Albasher G, Alarifi, S, 2020. Cyclophosphamide-induced oxidative stress and genotoxicity in murine bone marrow cells: A chemoprotective role of ascorbic acid. Oxid. Med. Cell. Longev. 2020: 3960843.

Flores-Flores A, Hernández-Abreu O, Rios MY, León-Rivera I, Aguilar-Guadarrama B, Castillo-España P, Estrada-Soto S, 2016. Vasorelaxant mode of action of dichloromethane-soluble extract from *Agastache mexicana* and its main bioactive compounds. Pharm. Biol. 54(12): 2807-2813.

Gałęska E, Wrzecińska M, Kowalczyk A, Araujo JP, 2022. Reproductive consequences of electrolyte disturbances in domestic animals. Biol. 11(7): 1006.

Gao X, Lin X, Wang Q, Chen J, 2024. Artemisinins: Promising drug candidates for the treatment of autoimmune diseases. Medicinal Research Reviews. 44(2): 867-891.

Ghosh S, Banerjee S, Sil PC, 2020. The beneficial role of curcumin on inflammation, diabetes and neurodegenerative disease: A recent update. Food Chem Toxicol.146: 111816.

Gungor H, Ekici M, Karatas O, Dik B, 2023. Protective effect of *Allium scorodoprasum* L. ethanolic extract in cyclophosphamide-induced hepatotoxicity model in rats. J. Pharm. Pharmacol. 75(5): 625-634. Hassanein EH, Kamel EO, Gad-Elrab WM, Ahmed MA, Mohammedsaleh ZM, Ali FE, 2023. Lansoprazole attenuates cyclophosphamide-induced cardiopulmonary injury by modulating redox-sensitive pathways and inflammation. Mol. Cell. Biochem, 478(10): 2319-2335.

Hossain A, Dave D, Shahidi F, 2020. Northern sea cucumber (*Cucumaria frondosa*): A potential candidate for functional food, nutraceutical, and pharmaceutical sector. Marine Drugs, 18(5): 274.

Huang XM, Zhang NR, Lin XT, Zhu CY, Zou YF, Wu XJ, Lan P, 2020. Antitumor immunity of low-dose cyclophosphamide: changes in T cells and cytokines TGF-beta and IL-10 in

mice with colon-cancer liver metastasis. Gastroenterol. Rep.8(1), 56-65.

Ijaz MU, Mustafa S, Batool R, Naz H, Ahmed H, Anwar H, 2022. Ameliorative effect of herbacetin against cyclophosphamide-induced nephrotoxicity in rats via attenuation of oxidative stress, inflammation, apoptosis and mitochondrial dysfunction. Human & Experimental Toxicol. 41: 09603271221132140.

Ismail GA, Gheda SF, Abo-Shady AM, Abdel-Karim OH, 2019. In vitro potential activity of some seaweeds as antioxidants and inhibitors of diabetic enzymes. Food Sci. Technol. 40: 681-691.

Kamyab E, Rohde S, Kellermann M Y, Schupp P. J, 2020. Chemical defense mechanisms and ecological implications of Indo-Pacific holothurians. Molecules. 25(20): 4808.

Kareh M, El Nahas R, Al-Aaraj L, Al-Ghadban S, Naser Al Deen N, Saliba N, Talhouk R, 2018. Anti-proliferative and anti-inflammatory activities of the sea cucumber *Holothuria polii* aqueous extract. SAGE Open Medicine. 6: 2050312118809541.

Khalilzadeh B, Shadjou N, Charoudeh HN, Rashidi M. R, 2017. Recent advances in electrochemical and electrochemiluminescence based determination of the activity of caspase-3. Microchimica Acta. 184: 3651-3662.

Kumar PS, Samriti F, Kumar MS, Pratibha M, Chandra GI, Mishra P, 2022. Hepatoprotective and antioxidant study of ethanolic extract of *T. cordifolia* against cyclophosphamide induced liver injuries. J Pharm Negat Results, 13(special issue 09): 6860-6872.

Lee J, Yang WS, Lee SY, 2016. The immunomodulatory properties of natural compounds from plants. Archives of Pharmacal Research. 39(11): 1554–1564.

Li J, Liu Y, Yuan J, Li X, Xu Z, Wang Q, 2025. Damage effect and mechanisms of cyclophosphamide to human neuroblastoma SH-SY5Y cells. Chin J Pharmacol Toxicol. 38(8).

Li L, Chen B, Zhu R, Li R, Tian Y, Liu C, Gao S, 2019. Fructus Ligustri Lucidi preserves bone quality through the regulation of gut microbiota diversity, oxidative stress, TMAO and Sirt6 levels in aging mice. Aging (Albany NY), 11(21): 9348.

Liang CA, Su YC, Lin SJ, Tsai TH, 2023. Risk factors for acute kidney injury after high-dose methotrexate therapy: a single-center study and narrative review. Eur. J. Clin. Pharmacol 79: 789-800.

Lixin X, Lijun Y, Songping H, 2019. Ganoderic acid A against cyclophosphamide-induced hepatic toxicity in mice. J. Biochem. Mol. Toxicol.33(4): e22271.

Mamede I, Escalante-Romero L, Celso DSG, Reis, PCA, Dacoregio MI, Alves AC, Stecca C, 2024. Immunotherapy plus chemotherapy versus chemotherapy alone as first-line treatment for advanced urothelial cancer: an updated systematic review and meta-analysis of randomized controlled trials. Clin. Genitourin. Cancer. 102154.

McGrath MS, Wentworth BJ, 2024. The Renin–Angiotensin System in Liver Disease. Int. J. Mol. Sci 25: 5807.

Mills KA, Chess-Williams R, McDermott C, 2019. Novel insights into the mechanism of cyclophosphamide-induced bladder toxicity: chloroacetaldehyde's contribution to urothelial dysfunction in vitro. Archives of Toxicol. 93: 3291-3303.

Mohamed ME, Saber SA, El-Kafrawy SB, Alabdein Nassar MZ, El-Naggar HA, 2024. Biotechnological Activities of *Holothuria papillifera* Mortensen, 1938 Inhabiting the Suez Gulf (Northern Red Sea), Egypt. Egypt. J. Aquat. Biol. Fish.,28(4).

Mona MH, Omran NE, Mansoor MA, El-Fakharany ZM, 2012. Antischistosomal effect of holothurin extracted from some Egyptian sea cucumbers. Pharm. Biol. 50: 1144-1150.

Moussa R, Wirawati I, 2018. Observations on some biological characteristics of *Holothuria polii* and *Holothuria sanctori* from Mediterranean Egypt. Egypt. J. Aquat. Biol. Fish. 6: 351-357.

Nian Q, Liu R, Zeng J, 2024. Unraveling the pathogenesis of myelosuppression and therapeutic potential of natural products. Phytomedicine. 132: 155810.

Olayoku A, Abdul-Azeez OO, Oyinloye B E, Oguntibeju OO, 2020. The inflammatory cascade in cyclophosphamide toxicity: targets for therapy. J Inflamm Res or J. Inflamm. Res. 13: 319–333.

Omran NE, Khedr AM, 2015. Structure elucidation, protein profile and the antitumor effect of the biological active substance

extracted from sea cucumber *Holothuria polii*. Toxicol. Ind. Health. *31*: 1-8.

Omran NE, Salem HK, Eissa SH, Kabbash AM, Kandeil MA, Salem MA, 2020. Chemotaxonomic study of the most abundant Egyptian sea-cucumbers using ultra-performance liquid chromatography (UPLC) coupled to high-resolution mass spectrometry (HRMS). Chemoecology. 30: 35-48.

Oyagbemi AA, Omobowale OT, Asenuga ER, Akinleye AS, Ogunsanwo RO, Saba AB, 2016. Cyclophosphamide-induced hepatotoxicity in wistar rats: the modulatory role of gallic acid as a hepatoprotective and chemopreventive phytochemical. Int. J. Prev. Med. 7: 51.

Ozupek NM, Cavas L, 2017. Triterpene glycosides associated antifouling activity from *Holothuria tubulosa* and *H. polii*. Reg Stud Mar Sci. 13:32-41.

Paget GE, 1964. Evaluation of Drug Activities. Pharmacomertrics, eds. Laurence and Bacharach, Academic Press, New York, 1: 133-166.

Park SH, Kim JH, Lee SJ, 2020. Herbal extracts in regulating renin-angiotensin system and preventing hypertension. J. Ethnopharmacol. 249: 112368.

Polak Y, van Dussen L, Kemper EM, Vaz FM, Klouwer FC, Engelen M, Hollak CE, 2024. The clinical and biochemical effectiveness and safety of cholic acid treatment for bile acid synthesis defects: a systematic review. Orphanet J. Rare Diseases. 19: 466.

Rajauria G, Abu-Ghannam N, Gupta S, 2016. Antioxidant and anticancer potentials of brown seaweed-derived compounds in cyclophosphamide models. Marine Drugs. 14: 89.

Rehman MU, Tahir M, Ali F, Qamar W, Lateef A, Khan R, Sultana S, 2012. Cyclophosphamide-induced nephrotoxicity, genotoxicity, and damage in kidney genomic DNA of Swiss albino mice: the protective effect of Ellagic acid. Mol. Cell. Biochem, 365: 119-127.

Rivera-Lazarín AL, Calvillo-Rodríguez KM, Izaguirre-Rodríguez M, Vázquez-Guillén JM, Martínez-Torres AC, Rodríguez-Padilla, C, 2024. Synergistic enhancement of chemotherapy-induced cell death and antitumor efficacy against tumoral T-cell lymphoblasts by IMMUNEPOTENT CRP. Int. J. Mol. Sci. 25(14), 7938.

Saeed NM, El-Naga RN, Abdallah DM, 2017. Caffeic acid phenethyl ester ameliorates acute lung injury caused by intestinal ischemia/reperfusion: Role of oxidative stress and inflammatory cytokines. Inflammation. 40: 1300–1309.

Saghir SA, Alharbi SA, Al-Garadi MA, Al-Gabri N, Rady HY, Olama NK, Abdulghani MA, Al Hroob AM, Almaiman AA, Bin-Jumah MJ, 2020. Curcumin prevents cyclophosphamideinduced lung injury in rats by suppressing oxidative stress and apoptosis. Processes. 8:127

Şengul E, Gelen V, Gedikli S, Ozkanlar S, Gur C, Celebi F, Cınar A, 2017. The protective effect of quercetin on cyclophosphamide- induced lung toxicity in rats. Biomed Pharmacother 92:303–307.

Shah RR, Subramanian S, Balaraman R, 2017. Cyclophosphamide-induced toxic effects and the ameliorative potential of antioxidants: A review. Drug Chem. Toxicol. 40: 149–158.

Shalaby MA, Hammouda AA, Saad MM, 2016. Amelioration of cyclophosphamide-induced kidney injury by antioxidant supplementation. Toxicol. Reports. 3: 1–9.

Silambarasan T, Manivannan J, Krishna Priya M, Suganya N, Chatterjee S, Raja B, 2014. Sinapic acid prevents hypertension and cardiovascular remodeling in pharmacological model of nitric oxide inhibited rats. PloS one, 9: e115682.

Srirangan P, Sabina EP, 2025. Protective effects of herbal compounds against cyclophosphamide-induced organ toxicity: a pathway-centered approach. Drug Chem. Toxicol, 1-43.

Subavathy P,Thilaga RD, 2016. GC-MS analysis of bioactive compounds from whole body tissue methanolic extract of *Cypraea arabica* (L. 1758). World J Pharm Res. 5: 800-6.

Sundaresan A, Harini R, Viswanathan Pugalendi K, 2012. Ursolic acid and rosiglitazone combination alleviates metabolic syndrome in high fat diet fed C57BL/6J mice. Gen. Physiol. Biophys. 31: 323.

Tawfiek UM, 2016. Histomorphological, histochemical and ultrastructural. Anatomia Histologia Embryologia, 37: 251–256.

Teng F, Wang H, 2025. Protective effects and metabolomics analysis of dihydromyricetin on cyclophosphamide-induced hepatotoxicity in mice. Pharmaceutical Science Advances, 100063.

Wang Y, Zang QS, Liu Z, 2019. Cyclophosphamide-induced cardiac and renal toxicity: Mechanisms and protective strategies. Toxicol. Letters. 309: 70–79.

Wingfield LK, Atcharawiriyakul J, Jitprasitporn N, 2024. Diversity and characterization of culturable fungi associated with the marine sea cucumber Holothuria scabra. PLOS ONE, 19: e0296499.

Zhang Y, Wang L, Liu Y, Zhang H, 2018. Protective effects of natural antioxidants on the renin-angiotensin system in experimental models of hypertension. Current Hypertension Reports. 20: 91.

Zhang Y, Zhang H, Zhang Y, 2015. Cyclophosphamide-induced nephrotoxicity: A review on its pathogenesis and preventive strategies. Renal Failure. 37: 1006–1011.

Zhao J, Zheng H, Sui Z, Jing F, Quan X, Zhao W, Liu G, 2019. Ursolic acid exhibits anti-inflammatory effects through blocking TLR4-MyD88 pathway mediated by autophagy. Cytokine. 123: 154726.